Field Monitoring of Atmospheric Icing Events - A Case Study

Adeel Yousuf, Pavlo Sokolov & Muhammad S. Virk
Arctic Technology & Icing Research Group
UiT – The Arctic University of Norway
Email: yousuf.adeel@uit.no

***Abstract*— Icing at high altitudes is a major concern for energy sector and infrastructure development. Many icing models exist to predict and analyse icing conditions based on physical or analytical models. This paper presents a field study of meteorological icing events to estimate the Liquid Water Content (LWC) and droplets Median Volume Diameter (MVD), based on ice load from a single cylinder ice collector instead of using multi cylinder ice collector. In this study, ISO 12494 is used to analyse the data from a field ice monitoring station installed in Arctic region of northern Norway. This meteorological station consists of various icing sensors, weather sensor and web camera. Multiple icing events are recorded and analysed with a focus to estimate LWC and MVD using accreted ice mass from single cylinder ice collector. It is noted that accuracy for MVD and LWC estimation can be improved by using smaller time windows of icing events.**

Keywords- Atmospheric icing; Meteorological data; Icing sensor; ISO-12494.

I. Introduction

Ice accretion poses significant challenges at high latitudes or in cold climatic regions around the world, affecting aviation, construction, and energy sectors. The ice accretion on aircraft can deteriorate its aerodynamic performance. Similarly, ice may accrete on suspension bridge structures that can pose a traffic safety risk resulting in long bridge closures [1]. Blade icing on wind turbines may incur Annual Energy Production loss of 2% – 30%, change the blade aerodynamics, damage onboard controllers and cause safety risk to nearby population due to ice shedding [2] [3]. Similarly, ice accretion on power lines can result in the tower collapse. There're multiple *direct* & *indirect* ways to detect icing on structure. Direct methods normally read on-site sensors or sense changes in different physical quantities (capacitance, vibrations, *etc.*), whereas indirect approaches make use of meteorological parameters such as temperature, dewpoint, *etc.* & apply different data analysis techniques to remotely evaluate ice presence. Extensive literature work is available on both ice detection methodologies [3]-[6]. This paper focuses on the indirect approach using ISO-12494 method for ice detection leading to the calculation of LWC and droplets' MVD. ISO-12494:(2001) formulates a standard for atmospheric ice modelling and field measurements. It suggests using a reference ice collector (0.5 m length, 30 mm diameter) of vertical (freely rotating) cylinder exposed to icing conditions (10 m.a.g.l.).

Better knowledge about ice loads helps to improve the design and safety of structures in icing conditions. Different researchers have used ISO 12494 methodology to estimate ice loads on structures. Hämäläinen *et al.* [7] calculated icing related wind energy production losses by developing Finnish Icing Atlas after combining datasets of NWP and ice-growth model of ISO-12494. Sokolov *et al.* [8] used ISO-12494 to estimate Liquid Water Content (LWC) values in multicylinder assembly for dry ice monitoring to draw comparison of volume weighted averaging & spectrum averaging of droplets. Molkoselkä *et al.* [9] implemented ICEMET cloud droplet and imaging sensor in icing wind tunnel to determine LWC and droplets Median Volume Diameter (MVD) for mixed icing conditions using ISO-12494 standard for single rotating cylinder. Han [10] presented scaling method technique to determine LWC for glaze/rime ice from experimental ice thickness measured using 3D laser scanner. Rydblom *et al.* [11] introduced a cost-effective solution to measure MVD & LWC using Droplet Imaging Instrument (DII) for weather station in Sweden and validated its performance for Supercooled Liquid Droplets (SLD).

This paper used a freely rotating single cylinder to model ice load on structure. For this purpose, a meteorological weather station was designed and installed in northern Norway at Linken Narvik mountain (1006 m.a.s.l.). The area is prone to icing events. The primary aim of using the meteorological and icing data on the reference collector is to employ the ISO 12494 standard to estimate the MVD and LWC values from the measured field meteorological data. The practical usage of the recovered values of MVD and LWC is that they can be used in the subsequent analysis for the purposes of icing load estimations, extreme value analysis and to build a "catalogue" of MVD/LWC values, which can be useful for the Weather Research Forecast (WRF) simulations in the local geographical conditions. While numerical modelling and laboratory experiments (using icing tunnel) are two other techniques to model/measure the extent of icing, field ice monitoring method used in this paper offers high accuracy but at the expense of cost and time.

Section-II of this paper describes the analytical modelling theory for the calculation of MVD & LWC in the light of ISO-12494 standard. Section-III provides a description of installed weather station, followed by the obtained results for field ice monitoring in Section-IV. A brief conclusion is presented in Section-V.

II. Analytical Model

Ice mass accumulation on the man-made onshore objects primarily comes from atmospheric icing, *i.e.*, in-cloud or precipitation icing. For both the in-cloud icing and freezing rain/drizzle, the process of icing originates from the impingement of the supercooled water droplets onto the object in question. The main equation in the analytical modelling of

 ISBN: 978-1-61208-917-1

icing, which describes the rate of icing per unit time is given as (ISO 12494, 2001):

$$\frac{dM}{dt} = \alpha_1 \alpha_2 \alpha_3 w A v$$

In this equation, otherwise known as "*Makkonen model*" [12], A is the cross-sectional area of the object (*with respect to the direction of the particle velocity vector, v; A = LD, where L is the length of the object in z-direction, and D is the characteristic length of the object, i.e., chord length, leading edge diameter, cylinder diameter, etc*.), w is the liquid water content, α_1 is the collision efficiency, α_2 is the sticking efficiency, α_3 is the accretion efficiency. The correction factors α_1, α_2 and α_3 represent different processes that may reduce dM/dt from its maximum value wAv [*the units of wAv term in the ISO 12494 standard are g/s (equivalent to the dimensions of dM/dt). The value of dM/dt = vAw is the theoretical maximum impingement rate*]. These correction factors vary between 0 and 1. Factor α_1 represents the efficiency droplets collision, i.e., it is the ratio of the flux density (*in this particular case it is the mass flux (flow) rate*) of the droplets that hit the object, to the maximum flux density, which is a product of the mass concentration of the droplets, w, and the velocity, v, of the droplets with respect to the object.

While under the ISO 12494 methodology, it is commonly assumed that for the supercooled water droplets, smaller in size than what can be classified as the Supercooled Large Droplets (SLD, with MVD (d) > 50 µm), the sticking efficiency α_2 is always equal to 1, meaning all impinging droplets stick on impact, the same may not be true for the accretion efficiency α_3. Consequently, if the value of α_3 is reduced from 1, the ice growth can be classified as "wet", meaning that there is some loss of mass flux due to runback water and water droplets shedding, before they freeze. In this case the glaze ice will be formed. If the value of α_3 is equal to 1, then all impinging droplet freeze on impact. While, in reality, the recorded icing events were a mix of wet and dry ice growth, the fundamental simplification has been made in this study that $\alpha_2 = \alpha_3 = 1$, i.e., all impinging droplets stick and freeze on impact. This is done in order to avoid the uncertainties, pertaining to the calculation of the iced surface thermodynamics, as the available measurement data may be insufficient for this purpose. Furthermore, since the Makkonen model equation described above has two unknowns (α_1 and w), and there is only one reference collector installed, the calculation procedure first starts with a "guess" of LWC content. For the purposes of this study the range of w is $0.01 < w < 8$ g/m^3. The algorithm first starts with a prescribed LWC and then attempts to find such a MVD value, which produces "optimum" value of α_1 to minimize the error. The algorithm continues to sweep through the rest of LWC values till the "optimum" value is found for both α_1 and w, which minimizes the modelling error of measured accreted ice mass M. Figure 1 describes flowchart functionality for this method.

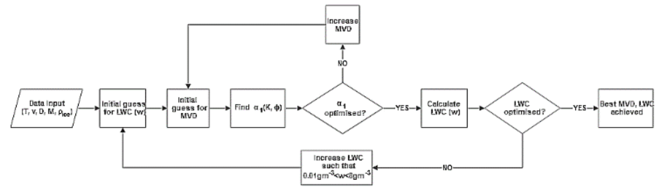

Figure 1. Method used in this study to estimate LWC and MVD

The overall collision efficiency α_1 is evaluated using the ISO 12494 formulae as:

$$E = A - 0.028 - C(B - 0.0454)$$

where constants A, B, and C are defined as:

$$A = 1.066K^{-0.00616}\exp(-1.103K^{-0.688})$$
$$B = 3.641K^{-0.498}\exp(-1.497K^{-0.694})$$
$$C = 0.00637(\phi - 100)^{0.381}$$

K and ϕ are the dimensionless droplet's inertia and Langmuir parameter (sometimes also referred as impingement parameter), respectively and they are given as:

$$K = \frac{2\rho_p r_p^2 u}{9\mu_f C} = \frac{\rho_p d_p^2 u}{18\mu_f C}$$
$$\phi = Re^2/K$$

In which C is the characteristic length of the object, in case of cylinder $C = R$, where R is the cylinder radius. As it can be seen from the equations above, by manipulating the MVD value d the necessary change in the values of α_1 is achieved.

III. FIELD ICE MONITORING STATION

The field ice monitoring station used in this study, consists of a Campbell CR1000- data logger, which is interfaced with multiple meteorological sensors: wind speed/direction sensor (Lambrecht EOLOS), IR based ice detection sensor (HoloOptics T44) and ice load sensor (SAAB/Combitech). The ice load sensor consists of a freely rotating, heated single cylinder as per ISO-12494 standard. The setup also includes a web camera which was focused on the ice load sensor for verification of detected icing event. Data is recorded at the online server of Volue Instrument Technology AS via GSM module with a resolution interval of 1 minute for all sensors and 30 min for the web camera. Meteorological observations include average air temperature (℃), wind speed (m/s), wind direction (degrees), icing presence (0/1), ice mass (g), ice mass increment from previous value (g) and relative humidity (%RH). A brief description of these sensors is provided in Table-1. This filed icing station (Figure 2) was installed in Arctic region of northern Norway at Linken Narvik mountain (1006 m.a.s.l.).

Figure 2. The installed weather station at Linken Narvik

TABLE 1. BRIEF DESCRIPTION OF SENSORS USED FOR ICE MONITORING WEATHER STATION IN THIS STUDY

Sensors		Parameter Measured	Specifications
HoloOptics T44		Ice Presence [Ice/No Ice]	Principle of operation: Presence of ice is indicated when 85%-95% of probe surface is covered with 0.01-0.03mm of ice. If <25% of probe surface is covered, icing indication stops
Lambrecht EOLOS		Air Temp RH Wind Speed / Direction	Air temp. resolution: 0.1℃ %RH resolution: 0.5% Wind direction resolution: 1° Wind speed resolution: $0.1ms^{-1}$
SAAB / Combitech Ice Monitor		Icing Mass	Analogue output (4-20mA); Accuracy: ±50g Resolution = 4g (Max: 10kg) Freely rotating cylinder length = 0.5m Its bearing is electrically heated at constant temp. of 1℃

Data collected from the weather station is sorted and analysed to detect meteorological icing events. Raw data for ice-mass (in kgm^{-1}) as observed by ice load monitor is *smoothed* using local regression with weighted linear least squares and a 2nd degree polynomial model. 15 data-points are taken as a span for calculating the smoothed values while assigning lower weight to outliers. The smoothed ice mass values are treated for calculating LWC & MVD using the ISO-12494. Sticking efficiency (α_2) and freezing efficiency (α_3) are taken as 1 to simulate dry growth measurement of ice.

Moreover, the increment of iced cylinder diameter is assumed to follow the following relationship:

$$D = \sqrt{\frac{(4 \times m)}{\pi \rho_{ice}} + D_{uniced}^2}$$

Here, 'm' represents ice-mass after applying *smoothing filter*, 'ρ_{ice}' is the ice density (*the constant value of 700 kgm^{-3} has been chosen for this study as it is deemed to be a "middle-point" between the soft and the hard rime ice types and typical type of ice present in this region*) and 'D_{uniced}' denotes original diameter of cylinder before experiencing icing (equal to 30 mm). Since ISO-12494 method gives better results for high wind speeds, so only those data-points are evaluated where corresponding wind speed > $3ms^{-1}$. Similarly, ice shedding events are also neglected.

IV. RESULTS

From the recorded data sets from icing station, icing events are classified as *long-term* if they span more than 3 hours, and *short-term* otherwise. For this purpose, the corresponding calculations for long-term icing events are made on 180 min interval, whereas short-term icing events are taken as whole. For analyzing the trend across different icing events, mean values of LWC, temperature, RH, ice mass are plotted against the icing event number. Visuals obtained from the camera are used to verify the detected icing events.

1) Icing Events – December 2020

One short-term & two long-term icing events were identified on 10th Dec 2021. Figure 3 shows the raw data results from all sensors against time (*Central European Summer Time; CEST*) for specified icing events, whereas mean values for these parameters including MVD are plotted. The temperature during the first icing event increased with time from –2.8 ℃ to –1.4 ℃ and wind speed varied between $0.6\ ms^{-1}$ – $6\ ms^{-1}$.

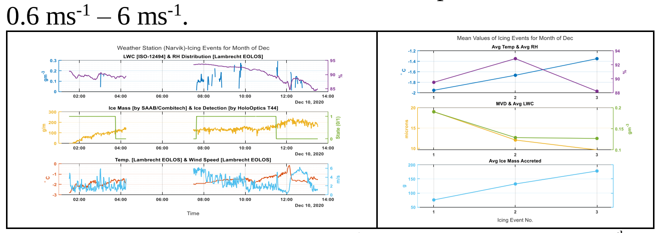

Figure 3. Meteorological data values for icing events detected on 10th December 2020

LWC could only be calculated at few data points during this event, where wind speed was around $5ms^{-1}$ but greater than $3ms^{-1}$ & RH > 90%. This is due to the constraint of K < 0.25 being reached for those points. Below this value the ISO 12494 is no longer valid and thus this data is filtered out. During second icing event ice mass rate appears to be slower than first & third events. HoloOptics ice sensor showed ice presence during all icing events but turned off for a portion of time as it can't detect icing thickness less than 0.01mm or when the probe surface is less than 25% covered with ice OR both. Two icing events are separated from each other in Figure 3 as there was a gap of around 3 hours. However, their average values are shown in the same figure to draw comparison among parameters. Timeline images in Figure 4 show the

 ISBN: 978-1-61208-917-1

accreted ice on ice-load monitor depicting a gradual increase in iced cylinder diameter. These images also verified the icing events detected from the meteorological data.

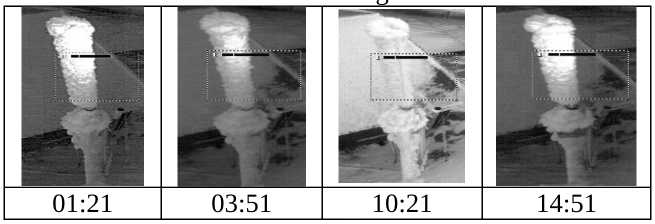

Figure 4. (Dec 10, 2020) Timeline of icing events recorded between 01:21—14:21 hrs. Dull light observed in an image captured on 14:51 is due to polar nights in Narvik during December.

2) *Icing Events – January 2021*

During the month of January 2021 a long icing event was observed starting from 14th Jan ,18:30hrs – 17th Jan 00:30 hrs. For analysis purpose, this icing event is divided into 18 short icing events, each one with the duration of 180 min (Figure 6: right image). Figure 5 shows the datasets for atmospheric temperature, relative humidity, calculated LWC, *etc.* against time, in addition to mean values of these parameters (including MVD) for corresponding icing event. While considering the ice mass and temperature in Figure 5 which almost continuously increased till the last icing event, high values of LWC are achieved when %RH > 90% and wind speed is around 5 ms^{-1}. It's more evident on 11:15—20:00 (15th Jan). The values of LWC in Figure 5 refer to ISO-12494 equations where it has been conditioned with wind speed in acceptable range (> 3ms^{-1}) and a positive change in ice mass; undefined LWC values against time fail either one or both the conditions. Infrared ice detection sensor remains turned on for whole duration defining it as a long meteorological icing event.

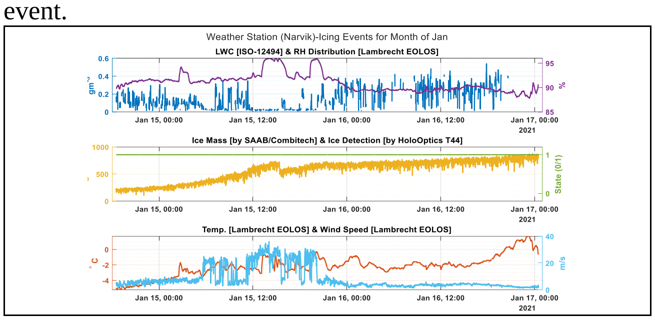

Figure 5. Meteorological data values for icing events detected from 14-17 January, 2021.

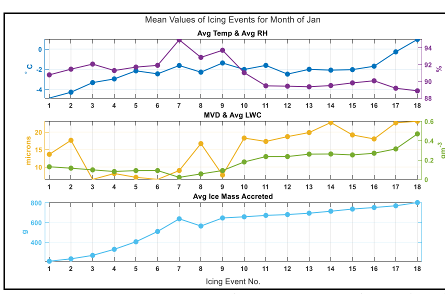

Icing Event #	Date/Time Range (Jan 2021)
1	14-Jan 18:31 – 14-Jan 21:30
2	14-Jan 21:31 – 15-Jan 00:30
3	15-Jan 00:31 – 15-Jan 03:30
4	15-Jan 03:31 – 15-Jan 06:30
5	15-Jan 06:31 – 15-Jan 09:30
6	15-Jan 09:31 – 15-Jan 12:30
7	15-Jan 12:31 – 15-Jan 15:30
8	15-Jan 15:31 – 15-Jan 18:30
9	15-Jan 18:31 – 15-Jan 21:30
10	15-Jan 21:31 – 16-Jan 00:30
11	16-Jan 00:31 – 16-Jan 03:30
12	16-Jan 03:31 – 16-Jan 06:30
13	16-Jan 06:31 – 16-Jan 09:30
14	16-Jan 09:31 – 16-Jan 12:30
15	16-Jan 12:31 – 16-Jan 15:30
16	16-Jan 15:31 – 16-Jan 18:30
17	16-Jan 18:31 – 16-Jan 21:30
18	16-Jan 21:31 – 17-Jan 00:30

Figure 6. (Jan 14-17)-[Left]: Mean temp/RH, droplets' MVD/ LWC & ice mass accreted on ice load monitor against different icing events. [Right]: Exact time divisions for icing events.

Examining the timeline images in Figure 7 shows rime ice appearance. A significant outer diameter change is observed for ice load monitor which allows to capture more striking droplets alongside an increase in %RH. Meanwhile taking ice-mass graph (in Figures 5, 6) into consideration, ice mass curve depicts a nonlinear increase for ice mass accumulation till 12:30 on 15th Jan after which the curve follows a linear fashion up till 17th Jan. %RH stayed above 90% for most of the time. Rest of the images show rime ice that apparently got hardened due to high wind speed and negative temperature on 15th Jan, possibly freezing the available captured water content.

Figure 7. Timeline of icing events recorded between Jan 14—Jan 16. The starting image on Jan 14 shows little icicles present on cylinder surface.

3) *Icing Events – February 2021*

A long-term meteorological icing event spanning about 18hrs is detected on 7th Feb. The event is subdivided into six small icing events, each one of 180min duration. Figure 8 shows the plots of different meteorological parameters based on data collected from sensors. Temperature change of approx. 1.5°C is observed during daytime which then again decreased till night. Relative humidity stayed close to 90% most of the time however high wind speed is observed ranging from 1.6 ms^{-1} – 12.8 ms^{-1}. Cylinder endures a slight increase in diameter as rime accretes, as can be seen in timeline images in Figure 9.

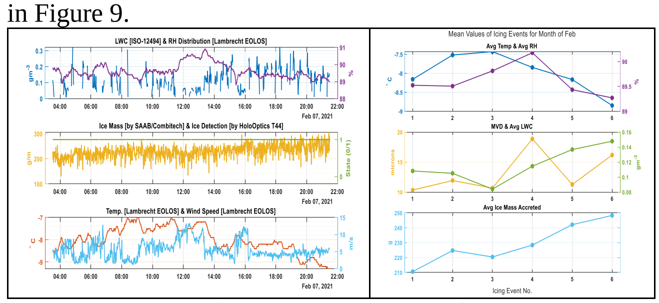

Figure 8. (Feb 7)-[Left]: Icing station data values for %RH/LWC, ice-mass/ice detection & temp./wind speed. [Right]: Mean temp/RH, droplets' MVD/mean LWC & ice mass accreted on Combitech ice-monitor against different icing events.

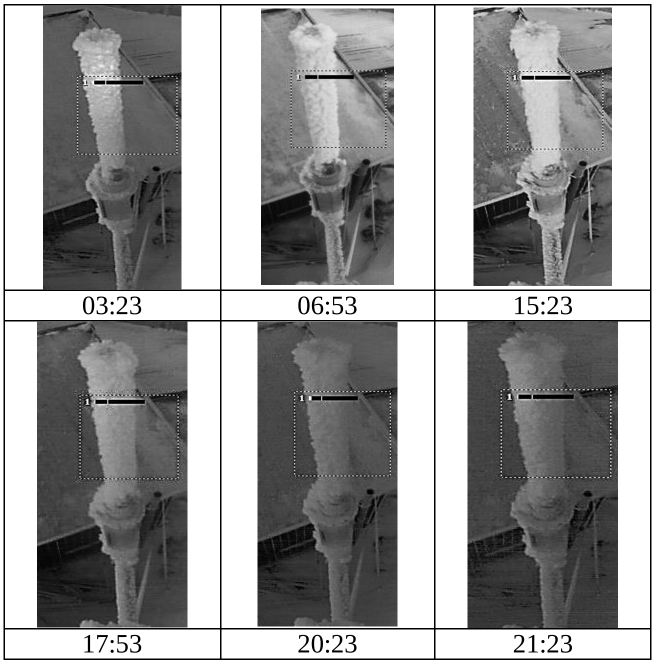

Figure 9. (Feb 7) Timeline of icing events recorded between 03:23—21:23

B. *Effect of Data Resolution*

Figure 3 showed ice accretion results on 10th Dec with 180min timespan for events 2 & 3. To assess how MVD accuracy changes with resolution of time window, same icing events (07:31-13:30) are subdivided into smaller 90min icing events. Figure 10 presents the comparison of mean values of temp., %RH, LWC, *etc.*

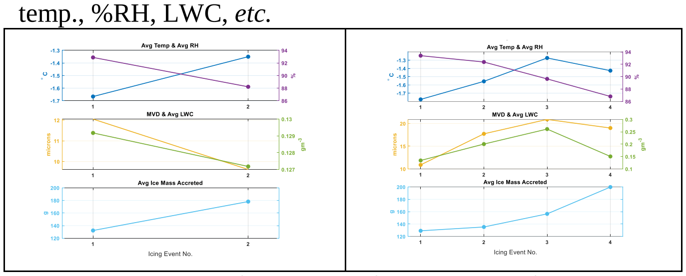

Figure 10. Comparison of mean values of icing parameters for a total icing duration of 6hrs (07:31-13:30) on 10th Dec. Left image displays results when icing duration is split into 2 icing events (comprised of 180min duration each), whereas right side image displays results when same duration is split into 4 small icing events (90min duration each).

It can be observed that improved results can be obtained with high resolution (i.e., splitting into smaller duration of icing events). MVD values have changed from (12, 9.6) µm to (10.8, 17.7, 20.9, 19) µm; similar is the case with other parameters. Increasing the resolution for icing event means studying fewer no. of droplets impinging the cylinder surface in a stipulated time, which removes potential outliers in data and gives better results but at the expense of more computation time.

V. Conclusion And Future Work

The paper presented an analytical method for ice modelling technique using field icing events data where a single cylinder assembly is used to estimate MVD and LWC. The method used in the study implemented ISO-12494 standard cylinder (0.5m in height, 30mm diameter) by Combitech as an ice load monitor. Analysis show that LWC and MVD can also be estimated using single cylinder ice collector instead of just using the multicylinder ice collector assembly. Multiple icing events were recorded and analysed. During analysis longer icing events spanning several hours of continuous ice accretion are subdivided into smaller events (3hrs). It was noted that accuracy for MVD and LWC can be improved by using smaller time intervals instead of longer intervals of icing events. As a future work the results can be further furnished to compare the accuracy using multi-cylinder network and assist the study of thermodynamics and heating phenomena in order to develop anti/deicing system. Due to high accuracy of field icing results, they can also be used to develop catalogues for Weather Research & Forecasting (WRF) simulations. Such measurements will provide a foundation for risk assessment during infrastructure development in Arctic region exhibiting similar climatic conditions.

Acknowledgment

The work reported in this paper is supported by the CoARICE project funded by Norwegian Research Council & NABL project funded by EU Kolarctic CBC.

References

[1] K. Kleissl and C. T. Georgakis, "Bridge ice accretion and de-and anti-icing systems: A review," in *The 7th International Cable Supported Bridge Operators Conference*, 2010. pp. 161-167

[2] S. Barber, Y. Wang, S. Jafari, N. Chokani, and R. S. Abhari, "The Impact of Ice Formation on Wind Turbine Performance and Aerodynamics," *Journal of Solar Energy Engineering,* vol. 133, no. 1, February 2011.

[3] K. Wei, Y. Yang, H. Zuo, and D. Zhong, "A review on ice detection technology and ice elimination technology for wind turbine," *Wind Energy,* pp. 433-457, 29 December 2019.

[4] U. N. Mughal and M. S. Virk, "Atmospheric Icing Sensors – An Insight," in *SENSORCOMM 2013: The Seventh International Conference on Sensor Technologies and Applications*, Barcelona, 2013. pp. 191-199

[5] U. N. Mughal, M. S. Virk, and M. Y. Mustafa, "State of the Art Review of Atmospheric Icing Sensors," *Sensors and Transducers,* vol. 198, no. 3, pp. 2-15, 31 March 2016.

[6] M. S. Virk, U. N. Mughal and G. Polanco, "Atmospheric Ice Accretion on Non-Rotating Vertical Circular Cylinder," *World Journal of Engineering and Technology,* vol. 3, no. 3, pp. 284-289, 2015.

[7] K. Hämäläinen and S. Niemelä, "Production of a Numerical Icing Atlas for Finland," *Wind Energy,* vol. 20, no. 1, pp. 171-189, 2016.

[8] P. Sokolov and M. S. Virk, "Modeling of Dry Ice Accretion on Cylinders – A Case Study of Present Analytical State," in *International Workshop on Atmospheric Icing of Structures (IWAIS)*, Reykjavik, 2019.

[9] E. Molkoselkä, V. Kaikkonen and A. Mäkynen, "Instrument and Method for Measuring Ice Accretion in Mixed-Phase

Cloud Conditions," in *IEEE Instrumentation and Measurement Technology Conference (I2MTC)*, Dubrovnik, 2020. pp. 1-5.

[10] Y. Han, "Theoretical and Experimental Study of Scaling Methods for Rotor Blade Ice Accretion Testing," The Pennsylvania State University, 2011.

[11] S. Rydblom, B. Thörnberg and E. Olsson, "Field Study of LWC and MVD Using the Droplet Imaging Instrument," *IEEE Transactions on Instrumentation and Measurement,* vol. 68, no. 2, pp. 614-622, February 2019.

[12] L. Makkonen, "Models for the growth of rime, glaze, icicles and wet snow on structures," *Philosophical Transactions of the Royal Society A: Mathematical, Physical and Engineering Sciences*, vol. 358, no. 1776, pp. 2913-2939, 2000.